

First lead isotopic data for cinnabar in the Almadén district (Spain): implications for the genesis of the mercury deposits

Primeros datos de isótopos de plomo en cinabrio del distrito de Almadén: Implicaciones en la génesis de los yacimientos de mercurio

P.L. Higuera⁽¹⁾, J. Munhá⁽²⁾, R. Oyarzun⁽³⁾, C.C.G. Tassinari⁽⁴⁾ y I.R. Ruiz⁽⁴⁾

⁽¹⁾ Departamento de Ingeniería Geológica y Minera. E.U.P. Almadén. Universidad de Castilla-La Mancha. Plaza Manuel Meca, 1. 13400 Almadén, Ciudad Real, España. pablo.higuera@uclm.es

⁽²⁾ Departamento/Centro de Geología. Faculdade de Ciências, Universidade de Lisboa. Lisboa, Portugal.

⁽³⁾ Departamento de Cristalografía y Mineralogía. Facultad de Ciencias Geológicas. Universidad Complutense. 28040 Madrid, España.

⁽⁴⁾ CPGeo, Instituto de Geociências. Univerdidade de São Paulo. São Paulo, Brasil.

ABSTRACT

The Almadén district constitutes the largest and probably the most intriguing mercury concentration in the world. This paper reports the first lead isotope compositions of cinnabar from the district. Whole samples and stepwise leaching cinnabar aliquots display relatively homogeneous isotopic compositions ($^{206}\text{Pb}/^{204}\text{Pb} = 18.112 - 18.460$; $^{207}\text{Pb}/^{204}\text{Pb} = 15.635 - 15.705$; $^{208}\text{Pb}/^{204}\text{Pb} = 38.531 - 38.826$). Taken together with Jébrak et al. (2002) pyrite lead isotope results, the new cinnabar isotopic data defines a steep array trend on the $^{207}\text{Pb}/^{204}\text{Pb} - ^{206}\text{Pb}/^{204}\text{Pb}$ diagram, suggesting a mixed contribution from both ancient upper continental crust and (enriched mantle derived) magmatic sources for the ores of the Almadén Hg deposits.

Keywords: mercury, Almadén, lead isotopes, upper continental crust, mantle

RESUMEN

El distrito de Almadén constituye la mayor y más enigmática concentración de mercurio del mundo. En este trabajo aportamos los primeros datos de geoquímica isotópica de plomo en cinabrio procedente de muestras del Distrito. Los resultados obtenidos muestran valores relativamente homogéneos ($^{206}\text{Pb}/^{204}\text{Pb} = 18.112 - 18.460$; $^{207}\text{Pb}/^{204}\text{Pb} = 15.635 - 15.705$; $^{208}\text{Pb}/^{204}\text{Pb} = 38.531 - 38.826$). Estos datos, junto con los aportados por Jébrak et al. (2004) para isótopos de plomo en piritas del mismo Distrito ponen de manifiesto una tendencia en diagramas $^{207}\text{Pb}/^{204}\text{Pb}$ vs $^{206}\text{Pb}/^{204}\text{Pb}$ que sugiere para los yacimientos del Distrito una contribución mixta a partir de corteza continental antigua y fuentes magmáticas derivadas de un manto enriquecido.

Geogaceta, 37 (2005), 67-70
ISSN:0213683X

Introduction and Geological Setting

The Almadén mercury mining district constitutes one of the largest geochemical anomalies on the Earth crust. The different mines of the district have produce almost one third of the total historic production liquid Hg metal, which is more than any other production of any other Hg mining district in the world. Mercury ore bodies are hosted by sedimentary and volcanic rocks belonging to a Lower Palaeozoic synclinal sequence that unconformably overlies the pre-Ordovician basement of the Central Zone of the Iberian Variscan Chain (Higuera, 1995; Hernández *et al.*, 1999). The volcanic-sedimentary rocks, ranging from Ordovician to upper Devonian in age, comprise several

packages of black shale and sandstone/quartzite units and include frequent intercalations of submarine mafic volcanics including the so-called *frailasca* rock, diatremes that locally cut the sedimentary and volcanic units (Saupé, 1990; Higuera, 1995). Mafic volcanism within the Almadén syncline was, by far, more important than elsewhere in the region; magmatic activity was almost continuous and evolved from earlier basanitic/nephelinitic and alkali-olivine basaltic extrusions, mostly into the Silurian-Devonian part of the section, to late tholeiitic intrusive dolerites, which are scattered throughout the whole sequence (Higuera and Munhá, 1993; Higuera, 1995). Basalts and dolerites underwent a long-term (427 - 365 Ma; Hall *et al.*, 1997; Higuera *et al.*, 2000a) regional

hydrothermal alteration, contemporaneous with water-cooling on the sea-floor, being pervasively transformed to albite-chlorite-carbonate rich spilites (Saupé, 1990; Higuera, 1995; Higuera *et al.*, 2000a); subsequently, the whole sequence was folded, weakly metamorphosed (Higuera *et al.*, 1995) and intruded at 305 Ma (Leutwein *et al.*, 1970) by felsic plutonic rocks during the Variscan deformation.

Two main types of Hg deposits have been described in the district (Hernández *et al.*, 1999): stratabound and discordant ore bodies. The former corresponds to well known Almadén type mineralizations, including the Almadén mine and the "El Entredicho" open pit, where the ore (cinnabar) is disseminated in lower Silurian quartzites (the so-called

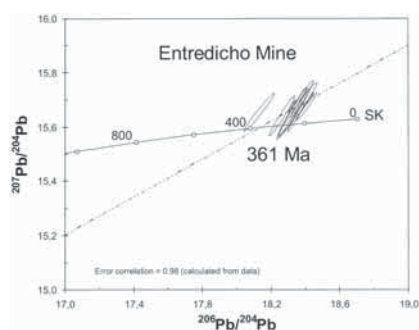


Fig. 1.- $^{207}\text{Pb}/^{204}\text{Pb}$ - $^{206}\text{Pb}/^{204}\text{Pb}$ diagram showing Stacey and Kramers (1975) model age isochron (SK) for El Entredicho cinnabar samples.

Fig. 1.- Diagrama $^{207}\text{Pb}/^{204}\text{Pb}$ - $^{206}\text{Pb}/^{204}\text{Pb}$ mostrando la isocrona modelo de edad de Stacey y Kramers (1975) para las muestras de cinabrio de El Entredicho.

Criadero quartzite). The second type (discordant deposits) are quite varied in the detail, and comprise small vein-type deposits in quartzitic rocks, as well as bigger deposits that can be described as epigenetic replacements in mafic volcanoclastic rocks such as Las Cuevas mine (Higueras *et al.* 1999). Despite the many differences in size and morphology between these two types of deposits, one feature is shared by both: they occur in close spatial association to *frailasca* rocks. The nature of mineralizing brines and ultimate origin of mercury has remained a matter of controversy; Saupé (1990) and Saupé and Arnold (1992) postulated the Ordovician black shales as the source of mercury, whereas Hernández *et al.* (1999) and Jébrak *et al.* (2002) suggested a relationship between the source of mercury and the alkali basalt volcanism in the area.

Lead Isotope Geochemistry

Analytical Procedures

Pb isotopic analyses of cinnabar and hydrothermally altered volcanic rock samples were carried out at Centro de Pesquisas Geocronológicas of University of São Paulo (Brazil). Because techniques to prepare cinnabar for lead isotope analysis are not easily available in the literature, the analytical procedures followed during this study will be described in detail. Ore samples were crushed and sieved to appropriate grain size (60 to 100 mesh) and cinnabar separation was done by electromagnetic separation; final purification (> 99%) was obtained by handpicking under a binocular microscope. For each sample, 300 mg cinnabar was ultrasonically washed in

triple distilled water, before chemical attack. Cinnabar was first dissolved using 3 ml of 6N HCl plus 2 ml of HNO₃, in a hot plate, at 100°C, during 24 hours. The evaporate was dissolved by 2 ml of 0.7N HBr and passed through an ion exchange column holding Dowex 1X8 AG anion exchange resin. After column treatment the solutions were brought to dryness and the residues were dissolved by 0.7N HBr and passed again through the same (Dowex 1X8 AG) ion exchange column as described above. Whole-rock volcanic samples were washed by HCl + HNO₃ and then totally dissolved in a mixture (2:1) of HF + HNO₃ using Parr type bombs; Pb was separated using HBr + HCl chemistry on Dowex 1X8 AG ion exchange resin. Lead was loaded onto a Re ribbon, using silica gel plus H₃PO₄ and analysed on a fully automatized VG 354 Micromass multicollector thermal ionization mass spectrometer. Analyses of a “National Bureau of Standards” standard NBS 981 yield a mass discrimination and fractionation correction of 1.0024 ($^{206}\text{Pb}/^{204}\text{Pb}$), 1.0038 ($^{207}\text{Pb}/^{204}\text{Pb}$) and 1.0051 ($^{208}\text{Pb}/^{204}\text{Pb}$); the combination of these uncertainties and within-run uncertainties are typically 0.15% - 0.48% for $^{206}\text{Pb}/^{204}\text{Pb}$, 0.13% - 1.07% for $^{207}\text{Pb}/^{204}\text{Pb}$ and 0.10% - 0.45% for $^{208}\text{Pb}/^{204}\text{Pb}$, all at 2s (95%) confidence level. The total Pb blank contribution, < 1 ng, is inconsequential. During the mass spectrometric analyses mercury was not detected; a superposition of a ^{204}Hg on the ^{204}Pb signal can therefore be excluded.

Two cinnabar samples from El Entredicho mine were further analysed by stepwise leaching, using a slightly modification of the technique described by Frei and Kamber (1995). Pure cinnabar (1.0 g) was submitted to the analytical procedures indicated in Table I.

Leached solutions were brought to dryness and then subjected to HBr chemistry on AG 1X8 ion exchange resin as described above.

Results

Jébrak *et al.* (2002) have reported lead isotope data on pyrite and sulphur

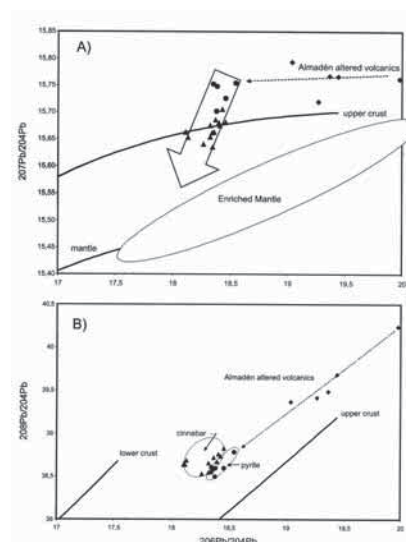


Fig. 2.- a, b) Diagrams of $^{206}\text{Pb}/^{204}\text{Pb}$ versus $^{207}\text{Pb}/^{204}\text{Pb}$ and $^{208}\text{Pb}/^{204}\text{Pb}$ for pyrites (filled circles; Jébrak *et al.*, 2002), cinnabar (filled triangles; Table II) and hydrothermally altered mafic volcanics (filled diamonds; Table II). Schematic location of “enriched mantle” (Wilson 1989) and Zartman and Doe (1981) “upper crust”, “lower crust” and “mantle” curves are also shown for comparison.

Fig. 2.- a, b) Diagramas $^{206}\text{Pb}/^{204}\text{Pb}$ vs $^{207}\text{Pb}/^{204}\text{Pb}$ y $^{208}\text{Pb}/^{204}\text{Pb}$ para piritas (círculos; Jébrak *et al.* 2002), cinabrio (triángulos; Tabla II) y rocas volcánicas máficas alteradas (rombos; Tabla II). Se muestra también de forma esquemática la localización de las curvas de “manto enriquecido” (Wilson, 1989), “corteza superior”, “corteza inferior” y “manto” (Zartman y Doe, 1981).

isotope data on pyrite and cinnabar from Nuevo Entredicho and El Entredicho deposits (Fig. 1). Lead isotopic data was obtained on pyrites from Nuevo Entredicho mine; relatively high $^{207}\text{Pb}/^{204}\text{Pb}$ ratios (15.70 – 15.75; Jébrak *et al.* 2002) were interpreted as lead that was re-mobilised from upper continental crust during Silurian-Devonian volcanic activity. Cinnabar sulphur isotopic values (+1.0 ‰ to +10.8 ‰) reported by Jébrak *et al.* (2002) are similar to that found by Saupé and Arnold (1992) for the Almadén deposit; $\delta^{34}\text{S}$ values correlate with the mercury/sulphur contents of the samples

Leached	Chemical treatment	time (Hs)	Temperature (°C)
L1	10 ml 1N HNO ₃	4	100
L2	10 ml 0.7N HBr	4	100
L3	10 ml 3N HCl	4	100
L4	10 ml 6N HCl	4	100
L5	10 ml 7N HNO ₃	4	100
L6	5 ml 6N HCl+ 5 ml 7N HNO ₃	4	100

Table I.- Physical-chemical procedures for cinnabar stepwise leaching.

Tabla I.- Procedimientos físico-químicos para la extracción secuencial de cinabrio.

(Jébrak *et al.*, 2002), suggesting that sulphur in the analysed cinnabar represents mixing of a low $d^{34}\text{S}$ magmatic source with a high $d^{34}\text{S}$ sedimentary source (Jébrak *et al.*, 2002).

Lead isotope analyses were performed on five cinnabar samples from El Entredicho (ETD 1, 2A, 2B) Las Cuevas (LC-10) and Almadén (ALMD-3) deposits. Five samples of hydrothermally metamorphosed mafic volcanics were also subjected to lead isotope analyses for comparative purposes. Lead isotope results are summarised in Table II. Cinnabar isotope values are fairly homogeneous, with a total range of $^{206}\text{Pb}/^{204}\text{Pb}$ from 18.112 to 18.460, $^{207}\text{Pb}/^{204}\text{Pb}$ from 15.635 to 15.705 and $^{208}\text{Pb}/^{204}\text{Pb}$ from 38.531 to 38.826. The lowest and the highest $^{206}\text{Pb}/^{204}\text{Pb}$ values are represented by Las Cuevas and Almadén cinnabar samples, with the latter also displaying the highest observed $^{208}\text{Pb}/^{204}\text{Pb}$ ratio (Table II); these subtle isotopic variations probably reflect the different settings of the Almadén and Las Cuevas deposits, being consistent with the complex, long-term, evolution of the hydrothermal system responsible for ore deposition in the Almadén mining district (see Higuera *et al.*, 2000a). Compared to lead isotope results on Nuevo Entredicho deposit pyrites (Jébrak *et al.*, 2002), the analysed cinnabar is less radiogenic relative to uranium lead (lower $^{206}\text{Pb}/^{204}\text{Pb}$ and $^{207}\text{Pb}/^{204}\text{Pb}$) but display similar $^{208}\text{Pb}/^{204}\text{Pb}$ isotopic compositions. All analysed hydrothermally altered volcanics ($^{206}\text{Pb}/^{204}\text{Pb} = 19.039 - 19.977$; $^{207}\text{Pb}/^{204}\text{Pb} = 15.720 - 15.794$; $^{208}\text{Pb}/^{204}\text{Pb} = 39.369 - 40.236$; Table II) are (at present) more radiogenic than both cinnabar and pyrite.

$^{207}\text{Pb}/^{204}\text{Pb} - ^{206}\text{Pb}/^{204}\text{Pb}$ cinnabar data plots close to the Stacey and Kramers (1975) model Pb-growth curve; regression of El Entredicho isotope data suggests incorporation of lead into cinnabar at ~ 361 Ma (Fig. 1), which is in accordance with Ar/Ar and Rb/Sr geochronological data (Hall *et al.*, 1997; Higuera *et al.*, 2000a) indicating a clustering of ages at 360 – 365 Ma for the hydrothermal activity associated with the Almadén Hg deposits.

The relative distribution of the Almadén volcanic rock isotope data, on uranium (Fig. 2a) and thorogenic (Fig. 2b) Pb isotope diagrams, (showing plumbotectonic curves of Zartman and Doe, 1981), suggests that Pb in these rocks were intensely re-homogenised by interaction with hydrothermal fluids, being now dominated by the same upper

sample	material	206/204	(2s)	207/204	(2s)	208/204	(2s)
ETD-2	cinnabar	18.266	0.061	15.641	0.060	38.531	0.062
ETD-2A4	cinnabar L4	18.132	0.073	15.653	0.057	38.684	0.059
ETD-2A5	cinnabar L5	18.399	0.006	15.680	0.006	38.667	0.006
ETD-2A6	cinnabar L6	18.326	0.067	15.654	0.073	38.543	0.069
ETD-2B1	cinnabar L1	18.429	0.016	15.705	0.017	38.730	0.017
ETD-2B2	cinnabar L2	18.346	0.040	15.635	0.043	38.555	0.043
ETD-2B3	cinnabar L3	18.370	0.044	15.686	0.045	38.714	0.046
ETD-2B4	cinnabar L4	18.409	0.047	15.675	0.041	38.757	0.044
ETD-2B5	cinnabar L5	18.324	0.018	15.675	0.019	38.654	0.019
ETD-2B6	cinnabar L6	18.342	0.087	15.662	0.087	38.550	0.088
ETD-1	cinnabar	18.357	0.092	15.663	0.081	38.577	0.083
LC-10	cinnabar	18.112	0.096	15.663	0.086	38.643	0.096
ALMD-3	cinnabar	18.460	0.016	15.681	0.016	38.826	0.017
SVC4/C10	volcanic	19.364	0.010	15.768	0.011	39.488	0.011
SNC1/C15	volcanic	19.266	0.012	15.720	0.012	39.419	0.012
LCPL2/17	volcanic	19.039	0.005	15.794	0.005	39.369	0.005
LCPL4/22	volcanic	19.440	0.014	15.767	0.014	39.687	0.014
LCPL2/18	volcanic	19.977	0.009	15.763	0.009	40.236	0.009

Table II.- Lead isotopic compositions of Almadén district hydrothermally altered mafic volcanic rocks from different locations, and cinnabar from El Entredicho (ETD), Las Cuevas (CL) and Almadén (ALMD) deposits (ETD-2A, 2B include results for stepwise leaching analysis -L).

Tabla II.- Composiciones isotópicas de muestras del distrito de Almadén. ETD: Cinabrio de El Entredicho; LC: Cinabrio de Las Cuevas; ALMD: Cinabrio de la mina de Almadén. Resto: rocas volcánicas basálticas afectadas por alteración hidrotermal. LI... indica extracción secuencial.

continental crust lead reservoir as indicated by Jébrak *et al.* (2002) for the Nuevo Entredicho pyrites. However, cinnabar data plots away from pyrite Pb isotopic values (Table II and Fig. 2a,b), implying that cinnabar lead must have incorporated a significant contribution from other than those upper continental crustal sources. Taken together with the Jébrak *et al.* (2002) lead isotope data, our results provide a case for mixing between different end member sources of Pb (Fig. 2a). The Pb isotopic data fall along a steep array that trends from the inferred composition of regional, upper crustal, hydrothermal fluids towards a lower $^{207}\text{Pb}/^{204}\text{Pb}$ component that could be ascribed to the primary magmatic lead in the volcanic rocks (as suggested by sulphur isotope data; Jébrak *et al.*, 2002). The end members for the Almadén sulphides are interpreted to lie on different growth curves representing reservoirs with different $^{238}\text{U}/^{204}\text{Pb}$; these are ancient upper crust (Jébrak *et al.* 2002) with relatively high $^{238}\text{U}/^{204}\text{Pb}$ and therefore relatively high $^{206}\text{Pb}/^{204}\text{Pb}$ and $^{207}\text{Pb}/^{204}\text{Pb}$ (Fig. 2a), and less radiogenic mafic magmas/upper mantle with lower (probably, variable) $^{238}\text{U}/^{204}\text{Pb}$. The absence of Pb isotopic data on fresh volcanic rocks from the Almadén district preclude a rigorous characterisation on the nature of the inferred mantle derived end member(s). However, a preliminary investigation of Sm/Nd isotopic systematics on seven samples of Almadén district mafic volcanics and ultramafic

xenoliths produced $^{143}\text{Nd}/^{144}\text{Nd}$ values from 0.512578 to 0.512757, with $e(\text{Nd})_{360}$ ranging from +2.5 to + 5.7. The inferred long-term LREE depleted mantle source(s) contrasts with the strong incompatible element enrichment seen in the Almadén mafic volcanic rocks (Higuera and Munhá, 1993; Higuera, 1995; Higuera *et al.*, 2000b), being consistent with geological and geochemical data (Hernández *et al.*, 1999) suggesting that rifting processes and plume related mantle metasomatic activity may have shortly predated the extensive mafic magmatism in the Almadén syncline during early Palaeozoic times. By pointing towards the involvement of those mantle derived magmatic sources of mineralization, the new cinnabar lead isotope data lends support to previous studies that proposed genetic relations between the Almadén mercury deposits and the regional alkali basalt magmatism (e.g., Higuera *et al.*, 2000b). Ortega and Hernández (1992) remarked compositional similarities between the ultramafic xenoliths at El Entredicho mine and the ultramafic rocks related to the Californian mercury deposits, and Fedorchuk (1974) has noted connections between mercury mineralization and ultramafic rocks elsewhere; moreover, many studies on mantle rocks (e.g., Clarke *et al.*, 1977; Irving, 1980; Dromgoole and Pasteris, 1987) emphasised close relationships between mantle metasomatism and sulphide mineralization. Thus, it is feasible that mantle metasomatic activity

and the low degrees of partial melting of Almadén magma (Higuera *et al.*, 2000b) could also provide for (either direct or indirect) Hg enrichment in the source rocks of Almadén deposits.

Conclusions

Whole samples and stepwise leaching cinnabar aliquots display relatively homogeneous isotopic composition ($^{206}\text{Pb}/^{204}\text{Pb} = 18.112 - 18.460$; $^{207}\text{Pb}/^{204}\text{Pb} = 15.635 - 15.705$; $^{208}\text{Pb}/^{204}\text{Pb} = 38.531 - 38.826$), being less radiogenic, relative to uranogenic lead, when compared to lead isotope results reported by Jébrak *et al.* (2002) for pyrites from Nuevo Entredicho deposit. Isotopic analyses for cinnabar from El Entredicho mine are grouped near the 360 Ma model age isochron (Stacey and Kramers, 1975), being consistent with both Ar/Ar illite ages recorded at Las Cuevas and El Entredicho mines (363 - 359 Ma; Hall *et al.*, 1997) and whole rock Rb/Sr geochronological data (365 ± 17 Ma; Higuera *et al.*, 2000a) reported for hydrothermal activity associated with the Almadén Hg deposits. The collective lead isotope data defines a steep array trend on the $^{207}\text{Pb}/^{204}\text{Pb} - ^{206}\text{Pb}/^{204}\text{Pb}$ diagram, suggesting a mixed contribution from both ancient upper continental crust (Jébrak *et al.*, 2002) and ("enriched" mantle derived) magmatic sources for the ores of the Almadén Hg deposits.

Direct observation (e.g., Prol-Ledesma *et al.*, 2002) and experimental evidence (Varekamp and Buseck, 1984; Fein and William-Jones, 1997) indicates that mercury transport in hydrothermal systems is largely promoted by reducing conditions under the presence of organic complexes. The close association of mercury mineralization and organic matter at Almadén suggests that mercury may have been transported in an organic phase. The Silurian black shales (with C_{organic} up to 7.64 wt%; Saupé, 1990) were probably the source of hydrothermal organic complexes, which formed by alteration and remobilization of indigenous organic matter. However, this does not forcedly imply that these rocks were the exclusive source of mercury (e.g., Saupé 1973). Indeed, the available stable and radiogenic isotope data on hydrothermal paragenesis (reviewed by Higuera *et al.*, 2000a, b) indicate that, except for a contribution to the carbon budget, there was no significant involvement of the sedimentary reservoir on the hydrothermal processes related to

Hg mineralization. Thus, considering all the available geological and geochemical data a deep-seated (mantle derived mafic magma) source of mercury is most probable. A contribution of mercury from the black shale, (which is likely to have been initially enriched in mercury by degassing of ascending magmas; Varekamp and Buseck, 1984; Rytuba and Herepoulos, 1992; Volkov *et al.*, 2002), cannot be excluded.

The present study lends further support to the hypothesis that the large accumulation of mercury at Almadén cannot be explained solely by leaching of regional sedimentary rocks. However, a combination of carbon leaching (from the sequence) and subsequent formation of Hg-organic complexes seems probable. In this respect we may finally suggest that huge deposits of Almadén formed because a combination of different, however related processes: 1) a deep seated source of mercury associated to the basaltic alkaline volcanism; 2) the development of widespread, convective hydrothermal activity; and 3) the leaching of organic matter from the black shales and formation of Hg organic complexes. The latter would have enhanced metal solubility, and promoted transport from and within the volcanic units.

Acknowledgements

This work was supported by grants POCA-PETROLOG: Centro de Geologia University of Lisboa, UI: 263; POCTI/FEDER (Portugal), and REN2002-02231/TECNO and PPQ2003-01902 (Spain).

References

- Clarke, D.B., Pe, G.G., MacKay, R.M., Gill, K.R., O'Hara, M.J. y Gard, J.A. (1977). *Earth and Planetary Science Letters*, 35, 421-428.
- Dromgoole, E.L. y Pasteris, J.D. (1987). *Geological Society of America Special Paper*, 215, 25-46.
- Fedorchuk, V.P. (1974). En: Congreso Internacional del Mercurio Barcelona, vol. 1, 117-143.
- Fein, J.B. y William-Jones, A.E. (1997). *Economic Geology*, 92, 20-28.
- Frei, R. y Kamber, B.S. (1995). *Earth and Planetary Science Letters*, 129, 261-268.
- Hall, C.M., Higuera, P.L., Kesler, S.E., Lunar, R., Dong, H. y Halliday, A.N. (1997). *Earth and Planetary Science Letters*, 148, 287-298.

- Hernández, A., Jébrak, M., Higuera, P., Oyarzun, R., Morata, D. y Munhá, J. (1999). *Mineralium Deposita*, 34, 539-548.
- Higuera, P. (1995). *Procesos petrogenéticos y de alteración de las rocas magmáticas asociadas a las mineralizaciones de mercurio del Distrito de Almadén*. Tesis Doctoral, Univ. de Castilla-La Mancha, 270 p.
- Higuera, P., Morata, D. y Munhá, J. (1995). *Boletín de la Sociedad Española de Mineralogía*, 18, 111-125.
- Higuera, P. y Munhá, J. (1993). *Terra Abstracts*, 5(6), 12-13.
- Higuera, P., Oyarzun, R., Lunar, R., Sierra, J. y Parras, J. (1999). *Mineralium Deposita*, 34, 211-214.
- Higuera, P., Oyarzun, R., Munhá, J. y Morata, D. (2000a). *Transactions of the Institution of Mining and Metallurgy*, 109, B199-B202.
- Higuera, P., Oyarzun, R., Munhá, J. y Morata, D. (2000b). *Revista de la Sociedad Geológica de España*, 13, 105-119.
- Irving, A.J. (1980). *American Journal of Science*, 280A, 389-426.
- Jébrak, M., Higuera, P., Marcoux, E. y Lorenzo, S. (2002). *Mineralium Deposita*, 37, 421-432.
- Leutwein, F., Saupé, F., Sonet, J. y Bouyx, E. (1970). *Geologische Mijnbouw*, 49-4, 297-304.
- Prol-Ledesma, R.M., Canet, C., Melgarejo, J.C., Tolson, G., Rubio-Ramos, M.A., Cruz-Ocampo, J.C., Ortega-Ororio, A., Torres-Vera, M.A. y Reyes, A. (2002). *Economic Geology*, 97, 1331-1340.
- Ortega, E. y Hernández, A. (1992). *Chronique Recherche Minière*, 506, 3-24.
- Rytuba, J.J. y Heropoulos, C. (1992). *U.S. Geological Survey Bulletin*, 1877, D1-D8.
- Saupé, F. (1973). *Sciences de la Terre (Nancy) Mém.*, 29, 342 p.
- Saupé, F. (1990). *Economic Geology*, 85, 482-510.
- Saupé, F. y Arnold, M. (1992). *Geochimica et Cosmochimica Acta*, 56, 3765-3780.
- Stacey, J.S. y Kramers, J.D. (1975). *Earth and Planetary Science Letters*, 26, 207-221.
- Varekamp, J.C. y Buseck, P.R. (1984). *Geochimica et Cosmochimica Acta*, 48, 177-185.
- Volkov, A., Sidorov, A.A., Goncharov, V.I. y Sidorov, V.A. (2002). *Geology of Ore Deposits*, 44(3), 159-174.
- Wilson, M. (1989). *Igneous Petrogenesis*. Unwin Hyman (London), 465 p.
- Zartman, R.E. y Doe, B.R. (1981). *Tectonophysics*, 75, 135-162.